5th International Conference on Biaxial/Multiaxial Fatigue and Fracture
Cracow'97, Poland

Didier DUPRAT*

A Model to Predict Fatigue Life of Aeronautical Structures with Out-of-Phase Multiaxial Stress Condition.

* Aéreospatiale Toulouse, France

Keywords : multiaxial fatigue, non proportional loading, out-of-phase loading.

ABSTRACT : A breadth of multiaxial fatigue research has been conducted under proportional in-phase loading. However, very little experimental work has been undertaken into order to establish the effects of out-of-phase loading on fatigue properties of materials and components. This paper presents a calculation methodology suitable for multiaxial out-of-phase stress loading. It is mainly based on the determination of local stress with finite elements computations and on the use of a multiaxial fatigue model. Predictions are compared with experimental results carried out a cross-shape test specimen. The correlation is excellent.

Notation

$\Sigma(t)$	Stress tensor
σ_{ij}	Component i,j of stress tensor
$\sigma_{ij_{mean}}$	Mean value of σ_{ij}
$\sigma_{ij_{alt}}$	Maximum half-amplitude of σ_{ij}, $\sigma_{ij_{alt}} > 0$
α_{ij}	Phase difference between the stresses σ_{ij}
ω	Frequency of loading
A_N, B_N	Positive constants defined for fatigue life N
T_{eq_a}	Equivalent shear stress amplitude
P_{mean}	Mean hydrostatic stress
p(t)	Hydrostatic stress
C_Σ	Load trajectory curve
S(t)	Deviatoric tensor
C_S	Load trajectory curve in the hyperplane of the deviatoric tensor
D	Longgest segment intercepting CS
p_e	Perimeter of the ellipse
N	Fatigue life
F1(t)	Loading in direction 1
F2(t)	Loading in direction 2
ϕ	Phase difference between $F_1(t)$ and $F_2(t)$

Introduction

Several multiaxial formulae have been proposed, such as those of Sines (1), Crossland (2), Dang Van (3) or Papadopoulos (4).

For periodical in phase loading, the predictions obtained using these equations comply with the experimental tendencies observed.

Phase difference between the stresses considerably reduces fatigue strength. Thus predictions are inclined to be over-optimistic and non conservative.

It is possible to formulate this loading as follows :

$$s_{ij} = s_{ij_{mean}} + s_{ij_{alt}} \cdot \sin(wt - a_{ij}) \qquad (1)$$

The purpose of this paper is to present a multiaxial model suitable for in-phase and out-of-phase loading. It is derived from Sines formula : results are identical in the case of in-phase loading.

Sines formula

The initial formula proposed by Sines is expressed as a linear combination of the equivalent shear stress amplitude and the mean hydrostatic stress reached during the cycle:

$$T_{eq_a} + B_N.P_{mean} < A_N \qquad (2)$$

Failure occurs when $(T_{eq_a}+B_N.P_{max})$ equals A_N.

Definition of P_{mean}

Hydrostatic stress p(t) equals a third of the trace of the stress tensor S(t).

$$P_{mean} = \frac{1}{2} \left[\max p(t) + \min p(t) \right] \qquad (3)$$

Definition of T_{eqa}

For any periodic load, the point representing the stress tensor S(t) describes a closed curve (C_S) which represents a load trajectory.

For radial (or proportional) loads, the load trajectory is a line segment passing through the origin. The principal axes of the stress tensor S(t) are fixed during the cycle.
In the most general case of periodical loads, the principal stress axes vary over time, as the load is not proportional. T_{eqa} is proportional to a distance in the hyperplane of the deviatoric tensor.

The projection of the load trajectory (C_S) onto the hyperplane of the deviatoric tensor is a closed curve (C_S) :

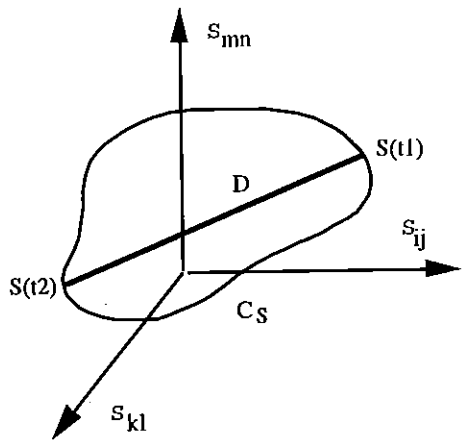

Figure 1. Load trajectory (C_S).

T_{eqa} is then expressed as: $$\boxed{T_{eqa} = \frac{1}{2}\frac{D}{\sqrt{2}}} \quad (4)$$

D is the length of the longgest segment intercepting (C_S). It is calculated as follows:

$$D = \max_{(t_1,t_2)} \sqrt{\text{trace}([S(t1)-S(t2)].[S(t1)-S(t2)])} \quad (5)$$

where: $S(t) = S(t)-p(t).Id$ $\qquad Id = \begin{bmatrix} 1 & 0 & 0 \\ 0 & 1 & 0 \\ 0 & 0 & 1 \end{bmatrix}$

Modification of the Sines formula

New Definition of T_{eq_a}

Considering an out-of-phase multiaxial stress load.

In the stress space, point M representing stress tensor S(t) is revealed as a closed curve which is an ellipse (figure 2). The projection of this ellipse in the deviatoric plane also results in an ellipse of long segment D/2 and short segment d/2.

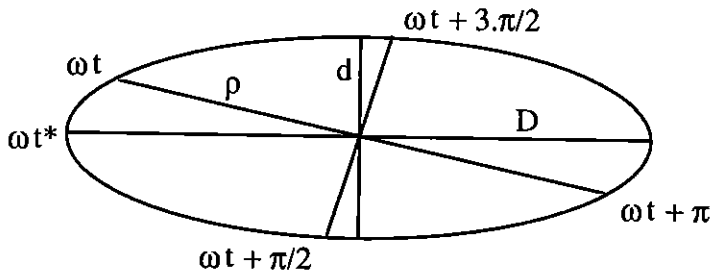

Figure 2. Projection of the load trajectory in the deviatoric plane

D et d are calculated with the following forms : $D = \max_{(t)} r(wt)$

$$d = \min_{(t)} r(wt)$$

$$\text{with } r(wt) = \sqrt{\text{trace}\left([S(t)-S(t+p)].[S(t)-S(t+p)] \right)} \qquad (6)$$

The deviatoric tensor is defined by the following relation : $S(t) = S(t) - p.Id$

The maximum or the minimum of r(wt) is obtained expressing the relation :

$$\frac{d}{dt} [r(wt^*)] = 0 \qquad (7)$$

Long segment D/2 is equal to the maximum of the two terms r(wt*)/2 and r(wt*+p)/2, short segment d/2 corresponds to the minimum.

In Sines original formula, only D is used in the calculation of the equivalent shear stress amplitude.

In order to take into account the totality of the phase difference (characterized by D and d), it is judicious to replace D by the half-perimeter of the ellipse : $p_e/2$.

T_{eq_a} is therefore formulated : $\boxed{T_{eq_a} = \frac{1}{2}\frac{p_e/2}{\sqrt{2}}}$ (8)

where : $\frac{p_e}{2} = \frac{p}{2}\frac{D+d}{2}\left[1+\frac{1}{4}\,l^2+\frac{1}{64}\,l^4+\frac{1}{256}\,l^6\right]$ and $l = \frac{D-d}{D+d}$ (9)

In the case of in-phase loading, $p_e/2$ is equal to D.

New Formulation of the multiaxial model

The two parameters of the model can be defined by means of two simple uniaxial tests. The tests selected here are a fully-reversed tension-compression test and a repeated tension (i.e. zero to tension) test.

For the fully reversed tension-compression test :

$$T_{eq_a} = \frac{s_{-1}(N)}{\sqrt{3}} \quad \text{and} \quad P_{mean} = 0 \qquad (10)$$

The Sines formula becomes : $\frac{s_{-1}(N)}{\sqrt{3}} = A_N$ (11)

Where $s_{-1}(N)$ is the stress amplitude corresponding to failure at N cycles.

• For the zero to tension test : $T_{eqa} = \frac{s_0(N)}{2\sqrt{3}}$ and $P_{mean} = \frac{s_0(N)}{6}$ (12)

The Sines formula becomes : $\frac{s_0(N)}{2\sqrt{3}} + B_N\frac{s_0(N)}{6} = A_N$ (13)

Where $s_0(N)$ is the maximum stress (i.e. twice the amplitude) corresponding to failure at N cycles. From equations (11) and (13) the parameters A_N and B_N are obtained :

$$A_N = \frac{s_{-1}(N)}{\sqrt{3}} \quad \text{and} \quad B_N = \sqrt{3}\left(\frac{2.s_{-1}(N)}{s_0(N)} - 1\right) \tag{14}$$

For economic reasons (weight and volume gain), calculations in civil aeronautics are generally made between low and high cycle fatigue, i.e. for lives on failure of between 10^4 and 10^7 cycles inclusive.

If, for this range of life, we plot experimental results, concerning an aluminium alloy, on a graph $(\log(s_{max}),\log(N))$, we can observe that these points fall approximately on a straight line (figure 3). From here on, it is possible to model fatigue cycle curves by means of straight lines.

The use of a specific point (corresponding to $N=10^5$ cycles) and the line gradient (-1/p) result in the following expressions:

$$s_{-1}(N) = s_{-1}(10^5).\left(\frac{10^5}{N}\right)^{1/p} \tag{15}$$

$$s_0(N) = s_0(10^5).\left(\frac{10^5}{N}\right)^{1/p} \tag{16}$$

Relations (15) and (16) are defined for a 50% probability of failure.
Introducing the above values of $s_{-1}(N)$ and $s_0(N)$ into Sines formula, we obtain:

$$T_{eqa} + \sqrt{3}\left(\frac{2.s_{-1}(10^5)}{s_0(10^5)} - 1\right) P_{mean} = \frac{s_{-1}(10^5)}{\sqrt{3}}\left(\frac{10^5}{N}\right)^{1/p} \tag{17}$$

Solving for N equation (17) the fatigue life is obtained :

$$N = 10^5.\left[\frac{\frac{s_{-1}(10^5)}{\sqrt{3}}}{T_{eqa} + \sqrt{3}\left(\frac{2.s_{-1}(10^5)}{s_0(10^5)} - 1\right) P_{mean}}\right]^P \tag{18}$$

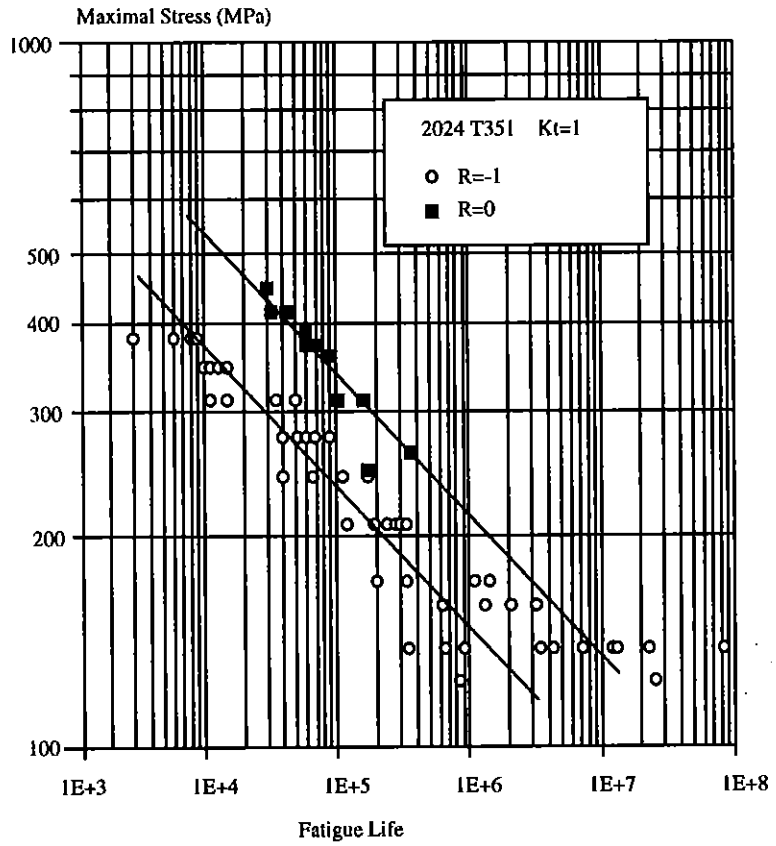

Figure 3. Fatigue results, 2024 T351

For the aluminium 2024 T351, the multiaxial fatigue model becomes:

$$s_{-1}(N) = 235.\left(\frac{10^5}{N}\right)^{1/5} \tag{19}$$

$$s_0(N) = 340.\left(\frac{10^5}{N}\right)^{1/5} \tag{20}$$

$$\boxed{N = 10^5.\left[\frac{135{,}5}{T_{eqa} + 0{,}66\, P_{mean}}\right]^5} \tag{21}$$

General approach

The approach presented is valid for in-phase and out-of-phase loading. Using discretised geometry, an elastoplastic computation gives the stress state at several instants during the load cycle. It is consequently possible to define, on one hand the mean hydrostatic stress, and on other hand the equivalent shear stress amplitude. Expression 18 is used to deduce fatigue life associated with each node of the finite element model.

Experimental validation

To validate this approach, we use a cross-shaped test specimen. It is subjected to a biaxial tension by means of a two actuators system fastened to a support.

The loading is defined as follow : $F_1(t) = F_{1moy}+F_{1alt}.\sin(wt)$

$$F_2(t) = F_{2moy}+F_{2alt}.\sin(wt-f)$$

with f = 0°, 30°, 45°, 60°, 90°, 120°, 150°, 180°

and $F_{1moy}+F_{1alt} = F_{2moy}+F_{2alt}$= 60000 daN

Analysis of test results highlights two crack initiation areas (see figure 6). For f<45°, crack initiation occurs in the fillet; for f>45°, in the skin close to the centre of the test specimen. We apply the approach described figure 4 : a finite element model gives the stress tensor at each node, and at several increments of load cycle. The theoretical crack initiation areas are in accordance with test results.

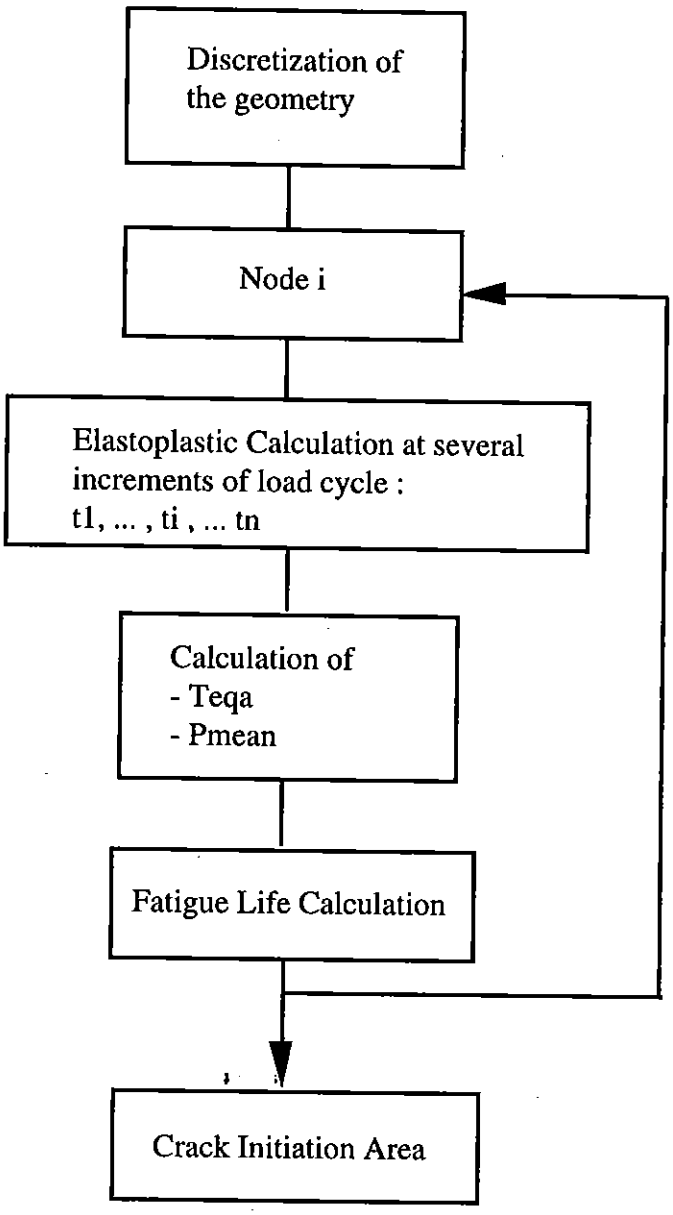

Figure 4. General Approach

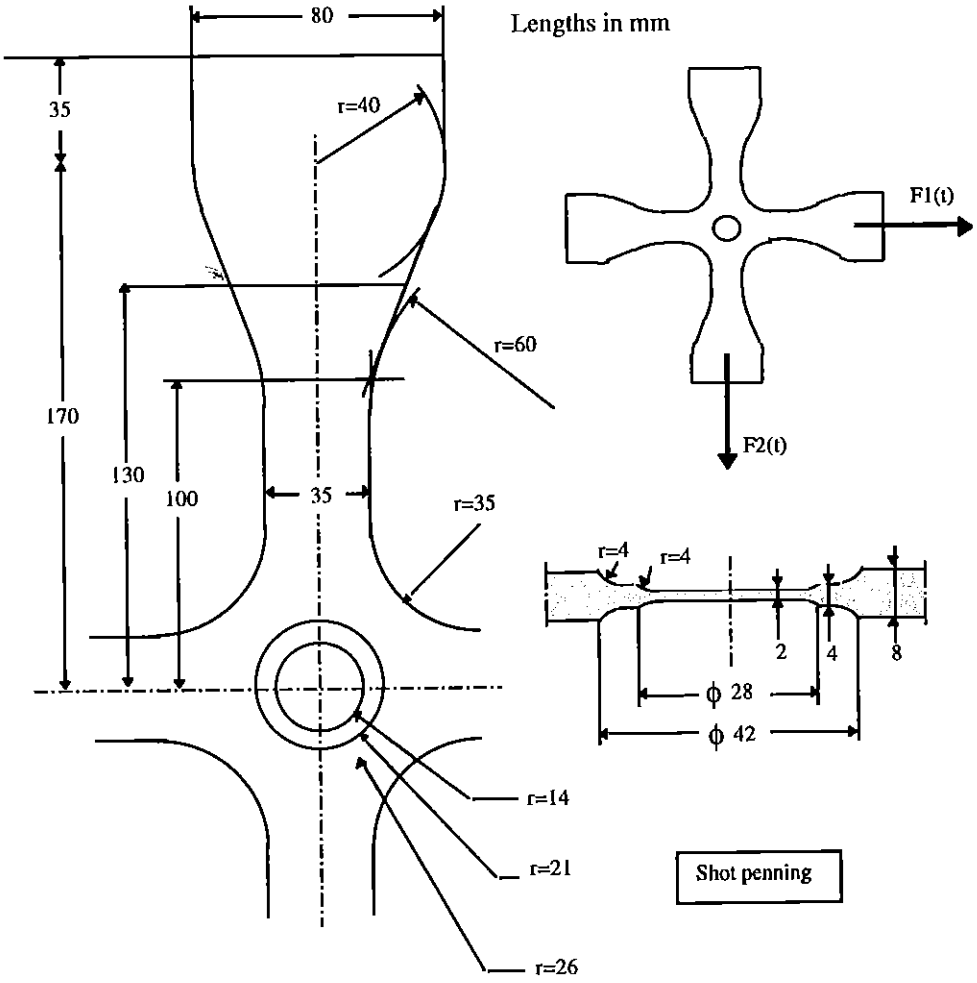

Figure 5. Test Specimen

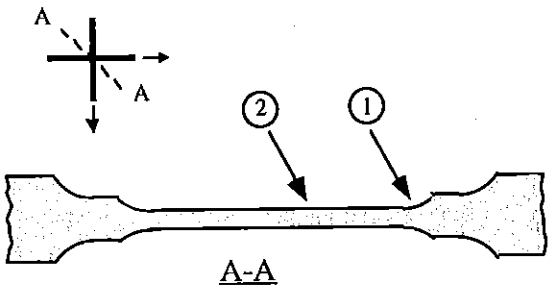

Figure 6. Crack initiation areas

Table 1. Test results

f	Fatigue Life	Crack Initiation area
0°	209900	1
0°	195870	1
0°	204240	1
30°	137015	1
30°	144163	1
45°	67067	2
45°	84305	2
60°	68074	2
60°	61811	2
90°	14760	2
90°	11715	2
120°	4465	2
120°	5768	2
150°	3630	2
150°	3745	2
180°	3147	2
180°	3524	2

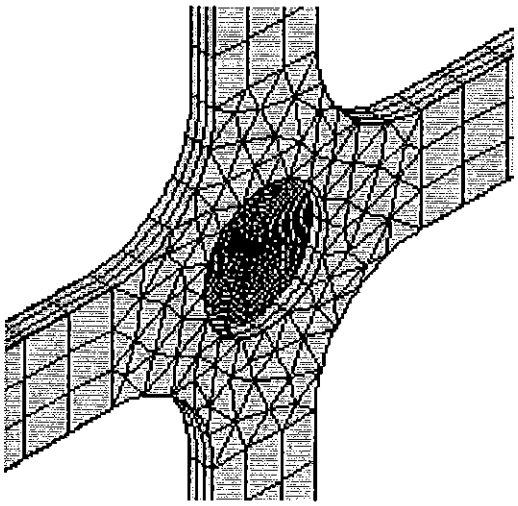

Figure 7. Finite element modelling

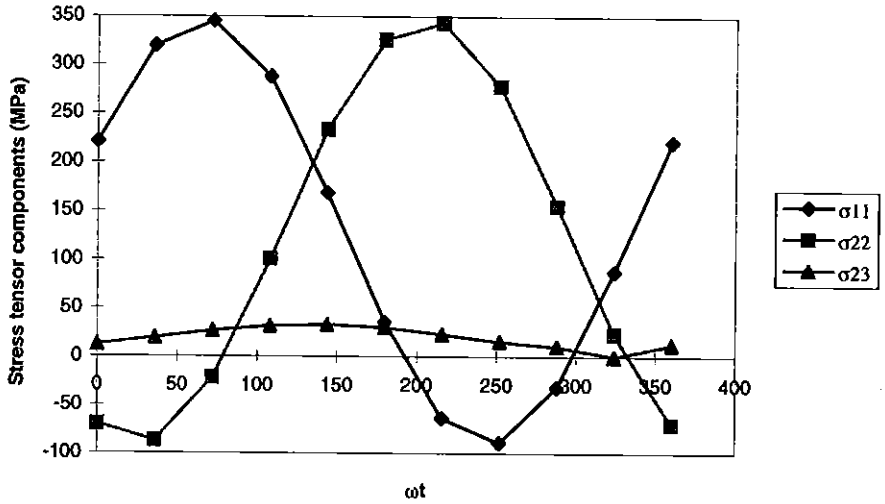

Figu 8. Stress tensor at several increments (f=90°)

Table 2. Stress tensor components

f	0°	30°	45°	60°	90°	120°	150°	180°
s_{11mean}	103,5	103,5	103,5	128	128	128	115	115
s_{22mean}	16	16	16	0	0	0	0	0
s_{33mean}	103,5	103,5	103,5	128	128	128	115	115
s_{12mean}	22	22	22	0	0	0	0	0
s_{13mean}	-22	-22	-22	0	0	0	0	0
s_{23mean}	48,5	48,5	48,5	20,5	20,5	20,5	20,5	20,5
s_{11alt}	84,5	93	102,6	169	217	257,6	260,7	264,5
s_{22alt}	13	12,5	11,9	0	0	0	0	0
s_{33alt}	84,5	93	102,6	169	217	257,6	260,7	264,5
s_{12alt}	18	24,9	30,9	0	0	0	0	0
s_{13alt}	-18	24,9	32	0	0	0	0	0
s_{23alt}	39,5	38,1	36,3	17	16,5	13	11,8	0
a_{22}	0	15	25	0	0	0	0	0
a_{33}	0	45	65	90	130	140	165	180
a_{12}	0	325	325	0	0	0	0	0
a_{13}	0	235	280	0	0	0	0	0
a_{23}	0	30	20	20	70	80	90	0

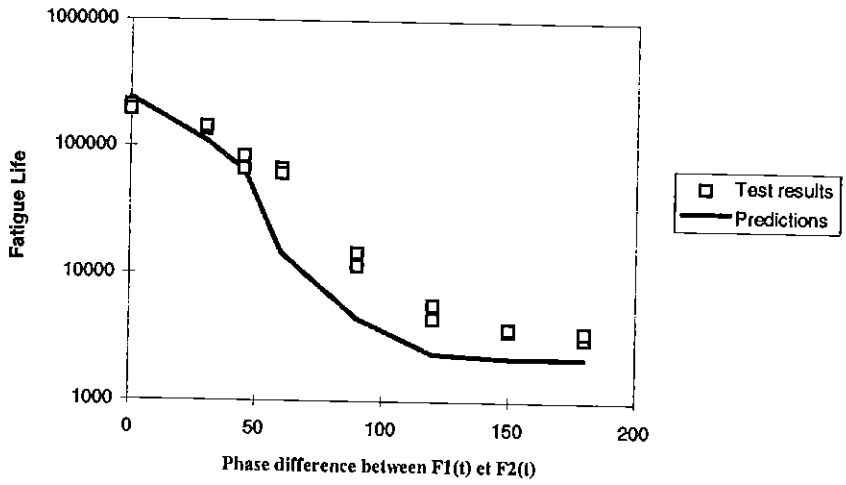

Figure 9. Comparison between test results and predictions

Conclusion

The calculation approach presented in this paper is efficient in estimating the fatigue life with in-phase and out-of-phase multiaxial stress condition.

It gives an excellent correlation with the tests. In addition, the predictions are conservative.

References

(1) Sines G. And Ohgi G., Trans. Am. Soc. Mech. Eng., J. Engng Mater. Techn., 1981, 103, pp 82-90.

(2) Crossland B., 'Proc. Int. Conf. Fatigue Metals', Institution of Mechanical Engineers, London, 1956.

(3) Dang Van K., Mém. l'Atillerie française, 1973, 3, pp 641-722,

(4) Papadopoulos I.V., Int. J. of Fatigue, 1994, 16, p377.